Available online at www.sciencedirect.com
SCIENCE DIRECT®
Journal of Theoretical Biology 234 (2005) 299–310
Journal of Theoretical Biology
www.elsevier.com/locate/yjtbi

Modeling allosteric regulation of de novo pyrimidine biosynthesis in *Escherichia coli*

Mauricio Rodríguez[a], Theresa A. Good[b], Melinda E. Wales[a,*], Jean P. Hua[a,1], James R. Wild[a]

[a]*Department of Biochemistry and Biophysics, Texas A&M University, 2128 TAMU, College Station, TX 77843-2128, USA*
[b]*Department of Chemical and Biochemical Engineering, University of Maryland, Baltimore County, 1000 Hilltop Circle, Baltimore, MD 21250, USA*

Received 12 July 2004; received in revised form 3 November 2004; accepted 17 November 2004

Abstract

With the emergence of multifaceted bioinformatics-derived data, it is becoming possible to merge biochemical and physiological information to develop a new level of understanding of the metabolic complexity of the cell. The biosynthetic pathway of de novo pyrimidine nucleotide metabolism is an essential capability of all free-living cells, and it occupies a pivotal position relative to metabolic processes that are involved in the macromolecular synthesis of DNA, RNA and proteins, as well as energy production and cell division. This regulatory network in all enteric bacteria involves genetic, allosteric, and physiological control systems that need to be integrated into a coordinated set of metabolic checks and balances. Allosterically regulated pathways constitute an exciting and challenging biosynthetic system to be approached from a mathematical perspective. However, to date, a mathematical model quantifying the contribution of allostery in controlling the dynamics of metabolic pathways has not been proposed. In this study, a direct, rigorous mathematical model of the de novo biosynthesis of pyrimidine nucleotides is presented. We corroborate the simulations with experimental data available in the literature and validate it with derepression experiments done in our laboratory. The model is able to faithfully represent the dynamic changes in the intracellular nucleotide pools that occur during metabolic transitions of the de novo pyrimidine biosynthetic pathway and represents a step forward in understanding the role of allosteric regulation in metabolic control.

Keywords: Pyrimidine biosynthesis; Metabolic modeling; Metabolism; *Escherichia coli*; Allosteric regulation

1. Introduction

The bacterium *Escherichia coli* is the most thoroughly studied microorganism, due primarily to its relative ease of manipulation in the laboratory and its extensively documented genetic and physiological organization. The amount of information and experimental data available on this enteric bacterium has made it the choice of a recently created alliance for cellular simulation, the International *E. coli* Alliance (Holden, 2002). The ultimate objective of this project is to create a virtual simulation of its cellular and molecular functions. This simulation will be comprehensive and capable of defining accurate responses to external manipulation in a way that reflects the in vivo metabolic functions and behavior of the living cell.

The functionally integrated, virtual *E. coli* is being constructed by combining currently available data with new directed research that is designed to augment accurate model building. Compilation and integration of several decades of molecular data is a monumental task in which this information has to be merged with

*Corresponding author. Tel.: +1 979 845 9459; fax: +1 979 847 9472.
E-mail addresses: m-wales@tamu.edu (M.E. Wales), j-wild@tamu.edu (J.R. Wild).
[1]Current address: NOTOCORD Systems, 113 Chemin de Ronde, 78290 Croissy, France.

0022-5193/$ - see front matter © 2005 Elsevier Ltd. All rights reserved.
doi:10.1016/j.jtbi.2004.11.023

that of genomics, transcriptomics and proteomics through step-wise mathematical simulations. The importance of simulating systemic metabolomics at the cellular level cannot be overstated. Understanding the interactions of all the cellular components will facilitate and guide future work, bringing a new level of understanding to how molecular life functions are integrated at the cellular level.

From the early work analysing sensitivity coefficients within a pathway (Schlosser and Bailey, 1990) to the more recent efforts to deal with the data pouring in from the *E. coli* genome sequencing project (Segre et al., 2003; Reed et al., 2003; Allen et al., 2003; Reed and Palsson, 2004), a growing need to integrate diverse experimental observations has resulted in the application of modeling as a powerful tool in the study of metabolic processes. Research has focused on cellular mechanisms of control such as the study of DNA replication (Hansen et al., 1991), regulation of transcription (Bremer et al., 2003; Covert and Palsson, 2002) and chemotaxis (Shimizu and Bray, 2002). Specific approaches have been applied to some metabolic pathways, as is the case of a model of attenuation in the tryptophan biosynthetic pathway (Koh et al., 1998) and the *lac* operon (Vilar et al., 2003). While many of the metabolic modeling efforts with *E. coli* have been focused on improving conditions for a desired commercial application (Kramer et al., 2003; Alvarez-Vasquez et al., 2002; Lee et al., 2002), more basic research has been performed on the metabolic pathways of different organisms (Raghunathan et al., 2004; Forster et al., 2003; Schilling et al., 2002). These and other works have contributed greatly towards a general understanding of the regulatory mechanisms of cellular networks and its applications. However, to our knowledge, there is no body of literature specifically dedicated to analysing *E. coli* metabolism from a pure description of the mechanisms controlling networks in a wild-type environment.

It is important to understand the detailed contribution and coordination of the diverse mechanisms controlling metabolic pathways. De novo nucleotide metabolism synthesizes purines and pyrimidines, the building blocks of nucleic acid polymers which constitute a fundamental component of the central metabolic processes of all living organisms. In *E. coli*, de novo pyrimidine synthesis begins with the condensation of ammonia or glutamine with bicarbonate and ends in the formation of UMP, UTP, CTP, dCTP and dTTP. Aspartate transcarbamoylase (ATCase, EC 2.1.3.2) and carbamoyl phosphate synthetase (CPSase, EC 6.3.5.5) are considered the key allosterically regulated enzymes controlling metabolic flux through the pathway. CPSase is feedback-inhibited by UMP and activated by ornithine, and ATCase, in turn, is inhibited by UTP and CTP and activated by the purine nucleotide ATP (Wales and Wild, 1999). The CPSase product, carbamoyl phosphate (CP), is shared by both the arginine and the pyrimidine biosynthetic pathways, establishing ATCase as the first step unique to pyrimidine de novo biosynthesis and its primary regulatory control.

To undertake the integration of a mathematical model of the de novo pyrimidine biosynthetic pathway, a system of coupled ordinary differential equations was formulated to describe the kinetic behavior of each of the enzymic reactions in the pathway. In the case of the allosterically controlled enzymes that initiate de novo pyrimidine biosynthesis, kinetic parameters were included to simulate the changes in activity induced by the allosteric effectors. In addition, the differential equations describing the biosynthesis of the first two enzymes in the pathway need to contain expressions for the decrease in enzyme synthesis in the presence of elevated pyrimidine nucleotide concentrations. As appropriate, the kinetic parameters for the model and the form of kinetic expressions for individual enzymes in the pathway were optimized from an extensive body of research in our laboratory and that published by others. In this study, an initial mathematical model of the regulation of de novo pyrimidine biosynthesis in *E. coli* is described. Underlying is the significant contribution that allosteric control puts into the rapid physiological adaptation of the cell to external stimuli and environmental changes.

2. Theory

2.1. Enzyme kinetics

As more genomes are sequenced, it becomes apparent that living systems are characterized not only by the complement of genes they carry but also by the mechanisms of control conducted at the molecular level. The most important intracellular molecules that are regulated include enzymes, intracellular substrate pools, allosteric ligand effectors, cofactors and, ultimately, the metabolic products. The ability of molecular systems to regulate the complex interactions among these molecules constitutes the basis of cellular homeostasis. The kinetics of the reactions catalysed by enzymes becomes the standard by which cellular metabolic systems have to reach and maintain metabolic steady-states.

Several parameters need to be considered when analysing enzyme kinetics: (1) the rate or maximum velocity of the reaction ($v_{\max}$) an enzyme can reach when it is saturated with substrate; (2) the Michaelis constant (K_M) or its equivalent ($S_{0.5}$) that equals the substrate concentration at which the rate of the reaction is half the $v_{\max}$; and (3) the turnover number (k_{cat}) or number of substrate molecules converted to products per second.

There are a variety of kinetic mechanisms, both homotropic and heterotropic, by which enzyme activities can be regulated. Substrates can affect the rate of a

reaction by cooperative interaction at the active site of an enzyme (homotropic effects), as can reaction products and other small molecules when present in adequate concentrations. In contrast, heterotropic effectors can change the kinetics by interaction at allosteric sites distinct from the active site. Under physiological conditions, substrate concentrations near their K_M facilitate the rapid adjustments of reaction rates. In some cases, there are mechanisms of homotropic cooperativity in which the affinity of interdependent catalytic sites is altered after a substrate molecule binds. Allosteric effectors, on the other hand, are present in a wide range of concentrations in the cell and they are readily available to bind to allosteric sites, causing structural rearrangements of the enzymes that may be transmitted as altered conformations of the active sites (Ricard and Cornish-Bowden, 1987). Intracellular concentrations of allosteric effectors provide an important form of metabolic regulation by providing a system that allows for rapid adjustments in biochemical flux by affecting the activity of one or more enzymes in the pathway.

The rates of individual enzymic reactions have been studied since the 19th century. Initial studies of Adrian Brown, Emil Fischer and others, were followed by the mathematical formulations proposed by Leonor Michaelis and Maud Menten in 1913 (Cornish-Bowden, 1997). The progress of a reaction showing typical hyperbolic first-order substrate saturation kinetics can be simulated by the following differential equation (Eq. (1)):

$$\frac{\mathrm{d}[A]}{\mathrm{d}t} = \frac{v_{\max} \times [A]_0}{K_M + [A]_0}, \tag{1}$$

where $[A]$ is the substrate concentration.

Even though it is relatively straightforward to formulate sets of simultaneous first-order nonlinear differential equations, the large number of parameters that need to be assigned makes it time-consuming and error-prone to manually perform the calculations. In the studies discussed here, the powerful differential equation solver of Mathematica™ (Wolfram Research Inc.) NDSolve was used. Using NDSolve to simultaneously solve arrays of differential equations through multistep integration methods, allows for successive points on a curve to be found with iterations of slope evaluation (Mulquiney and Kuchel, 2003).

To simulate the decrease in substrate concentration, an equation describing the relevant steady-state kinetic parameters ($v_{\max}$, K_M) and initial substrate concentration has been formulated. The Michaelis–Menten equation is traditionally used to show the time-dependence of substrate consumption and product formation of one such reaction. The numerical analysis and simulation of metabolic pathways comprising more complicated enzymic behavior is far more challenging.

2.2. Pyrimidine biosynthesis repression/derepression

When *E. coli* is grown under conditions of minimal supplied nutrients, most biosynthetic pathways are activated, including that of de novo pyrimidine biosynthesis. Growth under derepressing conditions will continue at steady state as long as the nutrient source and environmental conditions remain constant. In the case of pyrimidine biosynthesis, the addition of uracil to the media results in repression of the de novo pyrimidine pathway and production of pyrimidine nucleotides is maintained by the nucleotide interconversion or the salvage pathways. Under these conditions, de novo biosynthesis has been estimated to account for less than 20% of pyrimidine nucleotide production (Christopherson and Finch, 1978). It has been established that the level of the intracellular pools of CTP and UTP correlate with the levels of expression of the *pyr* genes (Jensen et al., 1984). As uracil is depleted, the concentration of enzymes involved in de novo biosynthesis returns to higher levels.

Derepression experiments were conducted with *E. coli* cells grown in minimal media supplemented with $50\,\mu g\,ml^{-1}$ uracil until they reached middle exponential growth levels ($\sim 8 \times 10^7$ cells ml^{-1}), as verified spectrophotometrically. Actively growing cells were quickly harvested by centrifugation and immediately resuspended in media without uracil. Nucleotide pools were extracted at the defined time intervals by sample precipitation with 6% trichloro-acetic acid and nucleoside triphosphates (NTPs) were separated and quantified using HPLC within 48 h after extraction (Wales et al., 1988).

Using this experimental approach in our laboratory has allowed us to demonstrate the physiological role that allosteric regulation of ATCase has in controlling flux through the de novo pathway. This type of information, in conjunction with the transitional dynamics of derepression, provides the essential metabolic parameters that must be detailed in a valid model.

3. Model development

Mathematically describing each individual enzyme is the necessary first step in the simulation of the flux through a metabolic pathway. The model described here has been developed to study the dynamic transitional effects of repression/derepression of pyrimidine biosynthesis. The de novo biosynthetic pathway, shown in Fig. 1, encompasses a series of nine reactions that lead to the production of UTP and CTP. CPSase (EC 6.3.5.5), ATCase (EC 2.1.3.2), dihydroorotase (DHOase, EC 3.5.2.3), dihydroorotate dehydrogenase (DHOdeHase, EC 1.3.3.1), orotate phosphoribosyl transferase (OPRTase, EC 4.1.1.23), and orotidine-5′-phosphate

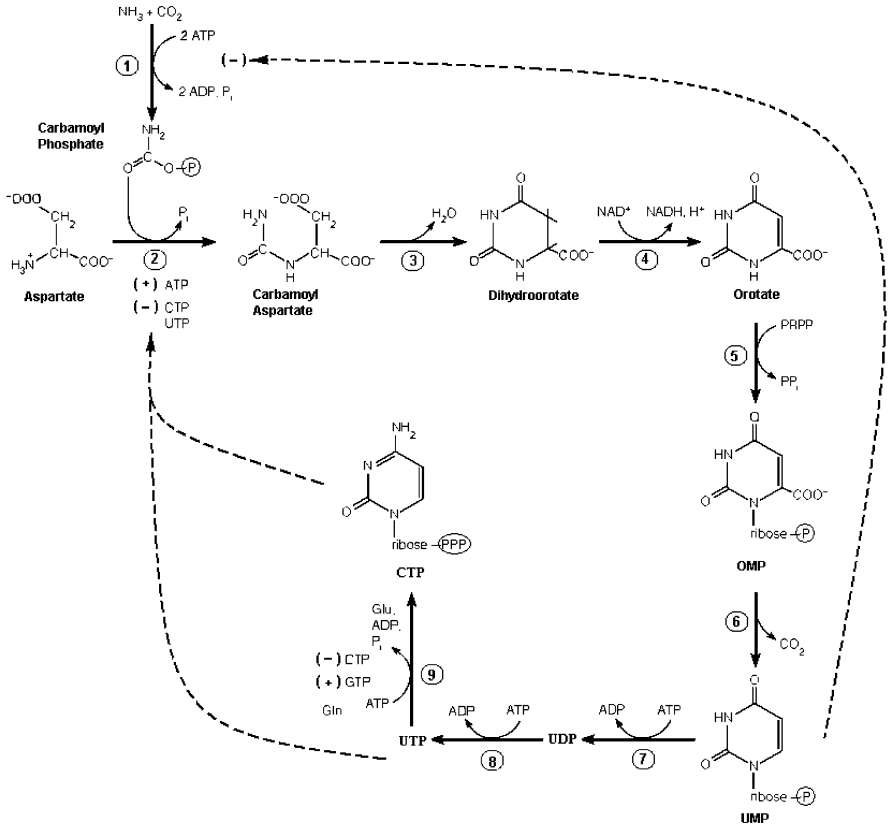

Fig. 1. Schematic representation of de novo biosynthesis in *E. coli*. The reactions catalysed by the pyr enzymes bring about the formation of UMP from aspartate, ammonia/glutamine, bicarbonate ATP and PRPP. Further reactions convert UMP to UTP and CTP. 1, carbamoyl phosphate synthase; 2, aspartate transcarbamoylase; 3, dihydroorotase; 4, dihydroorotate dehydrogenase; 5, orotate phosphoribosyl transferase; 6, orotidine-5′-phosphate decarboxylase; 7, uridylate kinase; 8, nucleoside diphosphate kinase; and 9, CTP synthase. The dashed arrow lines denote specific allosteric effects.

decarboxylase (ODCase, EC 2.4.2.10), catalyse the formation of UMP. UMP is phosphorylated to UDP by uridylate kinase (UMP kinase, EC 2.7.4.-) and UDP is subsequently transformed into UTP and CTP, through the action of nucleoside-5′-diphosphate kinase (NDKinase, EC 2.7.4.6) and CTP synthase (EC 6.3.4.2).

The definition of the mathematical functions, or rate equations, of the biochemical steps of this pathway must take into consideration the presence or absence of allosteric effects. In the first biochemical step (r_1), the reaction rate for the formation of CP, which is catalysed by CPSase (E_1), is described by Eq. (2). In this equation and all those following, the term $v_{\max i}$ refers to the apparent maximal velocity of the reaction *i*. Eq. (2) includes terms for the binding of bicarbonate (K_{bc}, K_{ibc}) and glutamine (K_q) and for the inhibitory effect exerted by UMP intracellular concentration (K_{iump}) (Rubino et al., 1986):

$$r_1 = \frac{v_{\max 1} E_1 \times bc \times glu}{(1 + ump/K_{iump})(K_{ibc} \times K_q + K_q \times bc + K_{bc} \times glu + bc \times glu)}. \quad (2)$$

CP condenses with aspartate in a reaction (r_2) to yield carbamoyl aspartate (CA), as described by

$$r_2 = \frac{v_{\max 2} E_2 + 2cp \times \frac{asp^{nH2}}{K_{t2}^{nH2}}}{\left(\frac{1}{1+atp/K_{atp}}\right)\left(1 + \frac{ctp}{K_{ctp}} + \frac{ctp \times utp}{K_{utp}}\right) + \left(\frac{K_{m2}^{nH1}}{cp} \times asp^{nH1} + cp \times \frac{asp^{nH2}}{K_{t2}^{nH2}}\right)}. \quad (3)$$

This reaction is catalysed by ATCase (E_2) and the mathematical expression includes a Hill coefficient (nH_1) that describes the cooperativity between the substrates and a second Hill coefficient (nH_2) for cooperativity under substrate inhibition (LiCata and Allewell, 1997). Additionally, a term for the allosteric effects is included. The rate of formation of CA is favorably affected by ATP, whereas CTP and UTP synergistically inhibit the enzyme.

The rate of change in concentration of CP is then given by the rate of its formation in reaction (1) minus the rate of its depletion in reaction (2), as seen in Eq. (4). An analogous expression can be developed for the rate of change of concentration of CA,

seen in Eq. (5)

$$\frac{d[cp]}{dt} = r_1 - r_2, \tag{4}$$

$$\frac{d[ca]}{dt} = r_2 - r_3, \tag{5}$$

where r_3 is the rate of formation of dihydroorotate from CA

$$r_3 = \frac{v_{max\,3} \times ca}{K_{m3} + ca}. \tag{6}$$

Analogous to r_3, the expressions for the remaining steps in the pathway are much simpler, as they do not include cooperativity or heterotropic interactions. Rather, as seen below, they follow simple Michaelis–Menten kinetics

$$\frac{d[dho]}{dt} = \frac{v_{max\,3} \times ca}{K_{m3} + ca} - \frac{v_{max\,4} \times dho}{K_{m4} + dho}, \tag{7}$$

where *dho* represents the dihydroorotate formed in the reaction catalysed by DHOase serving as substrate for the following reaction, catalysed by DHOdeHase

$$\frac{d[oro]}{dt} = \frac{v_{max\,4} \times dho}{K_{m4} + dho} - \frac{v_{max\,5} \times oro \times prpp}{K_{m5} + oro \times prpp}, \tag{8}$$

where *oro* and *prpp* are the substrates of the reaction catalysed by OPRTase

$$\frac{d[omp]}{dt} = \frac{v_{max\,5} \times oro \times prpp}{K_{m5} + oro \times prpp} - \frac{v_{max\,6} \times omp}{K_{m6} + omp}, \tag{9}$$

where *omp* is orotate-5′-phosphate

$$\frac{d[ump]}{dt} = \frac{v_{max\,6} \times omp}{K_{m6} + omp} - \frac{v_{max\,7} \times ump}{K_{m7} + ump} + \frac{v_{max\,9} \times ura \times prpp}{K_{m9} + ura \times prpp}, \tag{10}$$

where *ump* is the product yielded by the decarboxylation of *omp* by ODCase; and *ura* represents the external uracil incorporated into the cell from the culture media

$$\frac{d[utp]}{dt} = \frac{v_{max\,7} \times ump}{K_{m7} + ump} - \frac{v_{max\,8} \times utp}{K_{m8} + utp} - \frac{g_{pyr} \times ctp}{K_{Mp} + ctp}, \tag{11}$$

$$\frac{d[ctp]}{dt} = \frac{v_{max\,8} \times utp}{K_{m8} + utp} - \frac{g_{pyr} \times ctp}{K_{Mp} + ctp}, \tag{12}$$

where g_{pyr} and K_{Mp} are the pyrimidine utilization rate and constant of pyrimidine utilization, respectively. These two terms are based on the assumption that the UTP and CTP produced are part of an intracellular pool that is constantly used to supply metabolic demands. The products *utp* and *ctp* are formed by the action of the enzymes NDKinase and CTP synthase, respectively

$$\frac{d[ura]}{dt} = -\frac{v_{max\,9} \times ura \times prpp}{K_{m9} + ura \times prpp}. \tag{13}$$

In Eq. (10), there is a term for the synthesis of *ump* from uracil, when uracil is supplied in the external medium. Since experimental evidence indicates that an *E. coli* culture, upon changing the media from excess to absence of uracil, undergoes a metabolic adjustment that is reflected in the intracellular pools of NTPs, a simple expression for the degradation of the uracil was also included in Eq. (13).

In Eqs. (11) and (12), there are terms for the loss of UTP and CTP, respectively, as the nucleotides are incorporated into RNA. For both UTP and CTP, it was assumed that the rate of loss of NTPs into RNA was proportional to the growth rate of the organism as we assumed growth was limited by some other, external component. In future formulations of the model, the effects that the different NTP pools have on growth rate and the ability of the organism to adapt to different environments will be incorporated.

Since regulation of the pathway depends not only on biochemical regulation, but also on rates of synthesis and degradation of the CPSase and ATCase, expressions for the UTP- and CTP-dependent enzyme synthesis and enzyme degradation were included

$$\frac{d[E_1]}{dt} = \frac{K_{e1}}{(K_{e1} + ump) - k_{deg1} \times E_1}, \tag{14}$$

$$\frac{d[E_2]}{dt} = \frac{K_{e1} \times 60}{(K_{e2} + ctp + ura) - k_{deg1} \times E_2}, \tag{15}$$

where K_{e1} and K_{e2} are synthesis coefficients, and k_{deg1} is a degradation coefficient. These terms account for a simplification of additional genetic parameters involved in enzyme synthesis that are not included in this model. Importantly, however, the concentrations of the feedback regulatory molecules are also present in each of the expressions.

A total of 11 reaction rates and equilibrium expressions were formulated as differential expressions and integrated using the NDSolve algorithm (Mathematica™). Initial conditions were estimated, as described above, for steady-state conditions with a doubling time of 42 min.

3.1. Parameter estimation

Modeling cellular systems is a complex task and, often, metabolic networks have a large number of parameters in relation to the available experimental data. An attempt to precisely estimate all the parameters in a metabolic pathway involves tracing every independent variable over a large number of individual perturbation experiments. It is obvious that the techniques to achieve this for most metabolic networks are not currently available and, therefore, several parameters had to be computationally estimated. Kinetic parameters and relative enzyme and metabolite

Table 1
List of parameters used in the model

Parameter	Definition	Value	Reference
v_{max1}	v_{max} for carbamoyl phosphate synthetase	0.38 mmol l^{-1}	Calculated from Robin et al. (1989)
bc	Intracellular concentration of bicarbonate	8 mM	Estimated
glu	Intracellular concentration of glutamine	4 mM	Calculated from Neidhardt (1987)
asp	Intracellular concentration of aspartate	4 mM	Calculated from Neidhardt (1987)
prpp	Intracellular concentration of phosphoribosyl pyrophosphate	0.18 mM	Estimated
K_{ibc}	Bicarbonate inhibition constant	0.75 mol l^{-1}	Estimated
K_{iump}	UMP inhibition constant	0.98 mol l^{-1}	Estimated
K_{bc}	K$_M$ for bicarbonate	36 mM	Calculated from Robin et al. (1989)
K_q	K$_M$ for glutamine	22 mM	Calculated from Robin et al. (1989)
v_{max2}	v_{max} for aspartate	24 mmol l^{-1}	Calculated from LiCata and Allewell (1997)
K_{M2}	K_M for aspartate	19.8 mM	From LiCata and Allewell (1997)
K_{atp}	ATP binding constant	4.8 mM	Estimated
K_{ctp}	CTP binding constant	4.1 mM	Estmated
K_{utp}	UTP binding constant	4.9 mM	Estimated
$nH1$	Hill coefficient	2.3	From LiCata and Allewell (1997)
v_{max3}	v_{max} for dihydroorotase	24.7 mmol l^{-1}	Calculated from Jensen et al. (1984)
K_{M3}	K_M for dihydroorotase	0.7 mM	Estimated
v_{max4}	v_{max} for dihydroorotate dehydrogenase	6.4 mM l^{-1}	Calculated from Jensen et al. (1984)
K_{M4}	K_M for dihydroorotate dehydrogenase	0.24 mM	Estimated
v_{max5}	v_{max} for orotate phosphoribosyl transferase	0.6 mmol l^{-1}	Calculated from Jensen et al. (1984)
K_{M5}	K_M for orotate phosphoribosyl transferase	9.9 mM	Estimated
v_{max5}	v_{max} for OMP decarboxylase	0.8 mmol l^{-1}	Estimated
K_{M6}	K_M for OMP decarboxylase	32 mM	Estimated
v_{max7}	v_{max} for UMP kinase	1.18 mmol l^{-1}	Estimated
K_{M7}	K_M for UMP kinase	19.8 mM	Estimated
v_{max8}	v_{max} for nucleoside diphosphate kinase	0.28 mmol l^{-1}	Estimated
K_{M8}	K_M for nucleoside diphosphate kinase	8.4 mM	Estimated
v_{max9}	v_{max} for uracil phosphoribosyl transferase	2.8 mmol l^{-1}	Estimated
K_{M9}	K_M for uracil phosphoribosyl transferase	0.08 mM	Estimated
K_{i2}	Substrate inhibition coefficient for ATCase	2	Estimated
K_{deg1}	Degradation coefficient for CPSase	0.12	Estimated
K_{deg2}	Degradation coefficient for ATCase	0.072	Estimated
$nH2$	Second hill coefficient	2	From LiCata and Allewell (1997)
g_{rate}	Growth rate	42 min^{-1}	Measured
K_{Mg}	Coefficient for growth rate	396	Estimated
g_{pyr}	Pyrimidine utilization rate	0.4 min^{-1}	Estimated
K_Mp	Constant for pyrimidine utilization	5.8	Estimated
K_{e1}	Synthesis rate coefficient for CPSase	36	Estimated
K_{e2}	Synthesis rate coefficient for ATCase	120	Estimated

Summary of the parameters used to define the rate equations modeling the allosteric response on pyrimidine de novo biosynthesis in *E. coli*.

concentrations are listed in Table 1. Kinetic constants such as v_{max} and K_M were estimated from experimental data using standard techniques (Beale, 1988). In brief, an algorithm was developed which minimized the sum of the squares of the residuals between the output of the model (nucleotide concentration) and experimental data at discrete time points. The model consisted of the set of differential equations that describe the dynamics of pyrimidine biosynthesis. Model input parameters were the set of unknown kinetic constants. The local optimization was performed in Mathematica^{TM} via a built-in function (FindMinimum) which employed the following methods: Conjugate Gradient, Gradient, Levenberg-Marquardt, Newton and Quasi-Newton. As the solution was a local optimum, the parameter estimates obtained were dependent upon judicious choice of the initial conditions.

4. Model testing and validation

Whenever possible, individual estimates from the model were compared to available experimental data to validate the mechanistic steps in the model, forms of the mathematical expressions, and estimates of model constants. Several examples of model verification are described.

4.1. Case 1: CPSase

A step-wise validation of the model resulted in confidence that each of the differential equations was appropriately formulated. Validation was obtained by comparing the simulated results with available experimental data. Rate 1, shown in Eq. (2), represents the rate of CP synthesis by CPSase in the absence of other

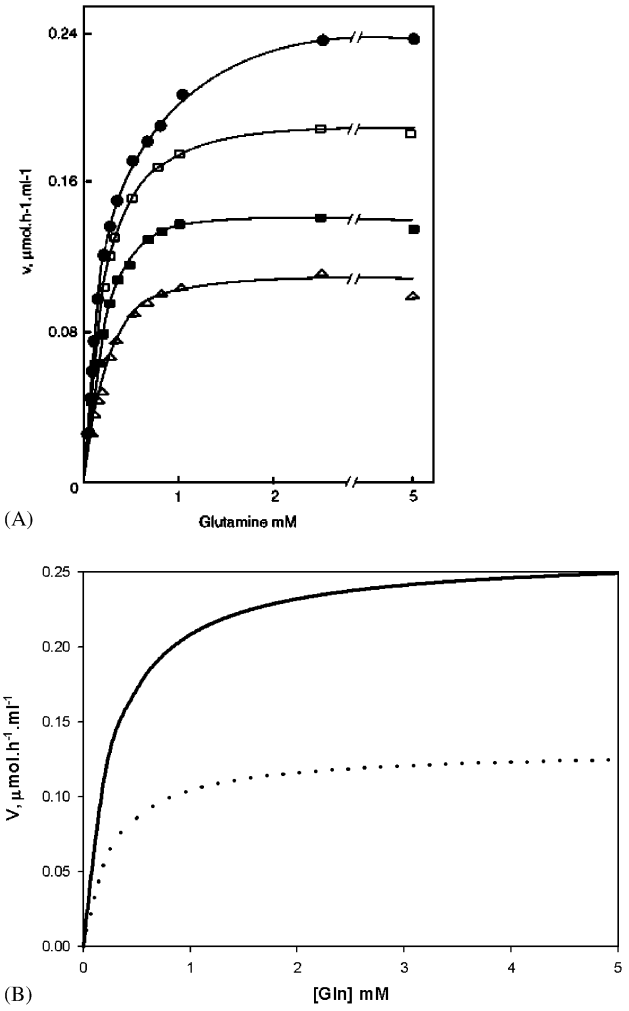

Fig. 2. Simulation of CPSase inhibition by UMP vs. experimental data. (A) Data published by Robin et al. (1989). No uracil added (●), 15 µg ml^{-1} (□), 25 µg ml^{-1} (■) and 50 µg ml^{-1} (△) of uracil. (B) Simulation of the rate of formation of CP as a function of the concentration of glutamine, both, in the presence of 50 µg ml^{-1} of UMP (· · · ·) and its absence (—).

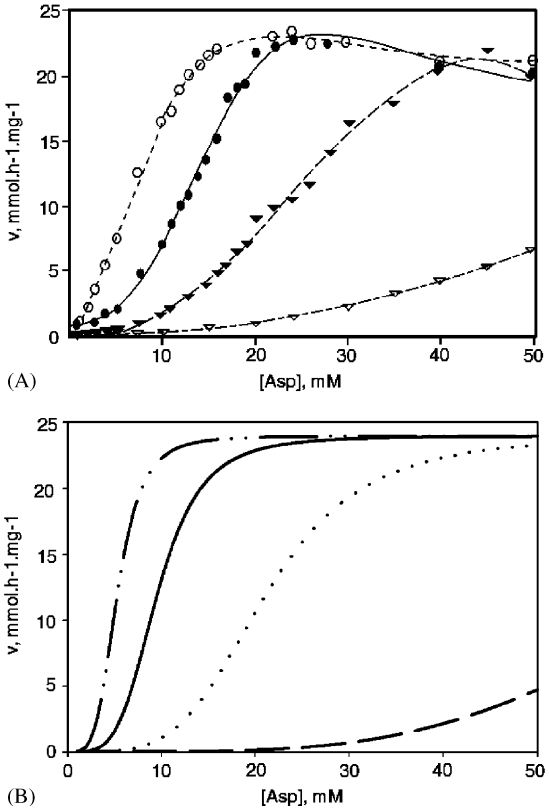

Fig. 3. Simulation of ATCase kinetic and allosteric behavior, compared to experimental data. (A) Saturation curves for ATCase unregulated (●) and its response to allosteric effectors: ATP (○), CTP (▼) and CTP + UTP (▽), as previously published by Wales and Wild (1999). (B) Mathematical simulation of the allosteric effects in ATCase: kinetic sigmoidal behavior in the absence of allosteric effectors (—); activation kinetics in the presence of ATP (· – ·); inhibitory effect by CTP (· · · ·); or UTP + CTP (– –).

enzymes in the pathway. The form of the equation mimics that of Michaelis–Menten but with an inhibition term included to account for the experimentally observed effects of UMP on CPSase activity. Simulation of the inhibitory effect of UMP on CPSase activity was achieved via this mathematical formulation as shown in Fig. 2. In the simulation, the reaction reaches saturation at approximately the same glutamine concentration as has been determined experimentally. In addition, the extent of the inhibitory effect is reproduced precisely as previously reported (Robin et al., 1989).

4.2. Case 2: ATCase

ATCase presents a more complex system given the multiple homotropic and heterotropic effects to which it is subjected. Previous studies have agreed on the cooperative behavior of substrate binding and the extent of allosteric effects induced by ATP, CTP, and UTP acting synergistically with CTP (Wild et al., 1989). The mathematical description of the enzymic reaction, rate 2, given in Eq. (3) accurately mimics all of these effects, as shown in Fig. 3.

4.3. Case 3: correlation between CPSase and ATCase enzyme levels and nucleotide pools

It has been established that the level of the intracellular pools of CTP and UTP correlate with the levels of expression of the *pyr* genes (Jensen et al., 1984); thus, the proposed model should accurately couple CTP and UTP levels with synthesis and degradation rates of the relevant enzymes. As seen in Eqs. (14) and (15), while the enzyme synthesis rate, the first term in each expression, is reduced in the presence of UMP and CTP, degradation of enzymes remains constant. Fig. 4 illustrates the changes in the UMP, CTP and UTP

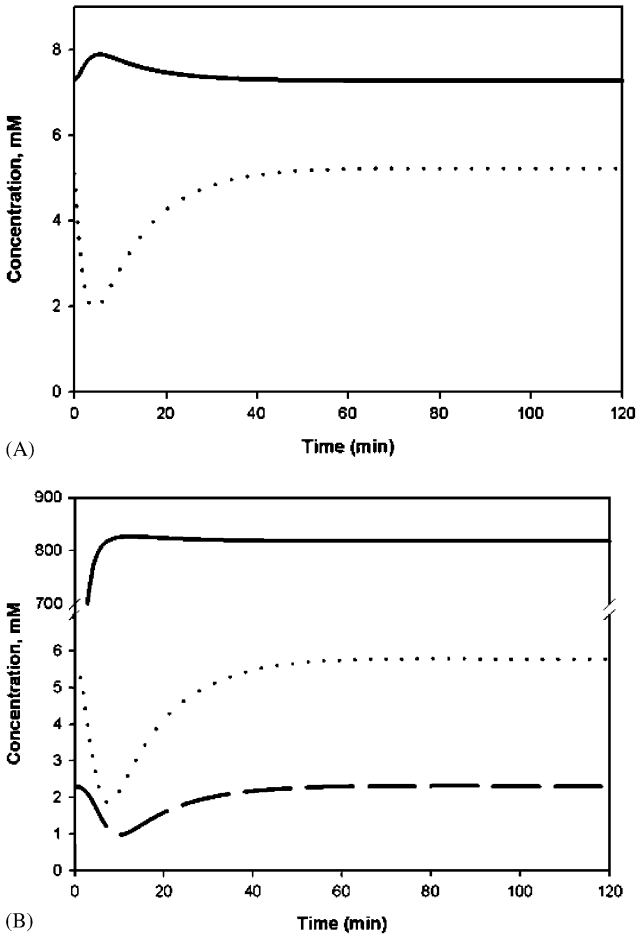

Fig. 4. Nucleotide levels change in the cell and the accompanying dynamic response of enzymes 1 and 2 (CPSase and ATCase, respectively). (A) UMP levels in response to derepression (· · · ·) and the corresponding response in CPSase levels (—). (B) UTP (· · · ·) and CTP (– –) derepression levels and the corresponding overexpression response of ATCase (—).

levels in the cell and the accompanying dynamic response of enzymes 1 and 2 (CPSase and ATCase, respectively).

4.4. Case 4: repression and derepression of CTP and UTP

Typically, the repression/derepression transition of the pyrimidine pathway enzymes causes a change in the size of the NTP pools. After the perturbation, CTP and UTP pools drop rapidly due to depletion. CTP levels drop to 66% and 46% their initial level for the allosterically regulated vs. the unregulated enzyme, respectively. UTP drops to 51% and 30%. As the pyrimidine pathway derepresses, the intracellular concentrations of UTP and CTP recover to their normal levels. Fig. 5 shows the dynamic response of the model to an initial high level of uracil that is rapidly consumed. Experimentally, this was achieved by taking repressed cells to a derepressed state by removing the uracil from the medium. Our model satisfactorily simulates the derepression behavior observed under these conditions. In addition, by simply removing the allosteric effect terms of ATP, UTP and CTP in rate 2, a second model was created that mimics the behavior of the cell without allosteric control of the second enzyme in the pathway (just catalytic subunits). Comparison of model predictions with and without allosteric subunits in the enzymes (holoenzyme and catalytic subunit simulations, respectively) qualitatively captures the experimentally observed differences in dynamic response of nucleotide pools in wild-type cells and those with their allosteric subunits deleted. As seen in Fig. 5, response of cells deficient in allosteric control is more dramatic compared to those with allosteric control. The complexity of the interrelation of all the equations makes this a finely tuned and sensitive model. Subtle changes in the kinetic parameters are being tested and used to predict outcomes of changes in experimental conditions.

5. Discussion

Several models have been published describing different metabolic pathways in *E. coli*, beginning with models 15 years ago describing the whole cell, but omitting control of metabolic pathways (Schlosser and Bailey, 1990). Currently, there are several models that describe specific pathways in *E. coli* such as the tryptophan biosynthetic pathway (Koh et al., 1998), replication (Hansen et al., 1991), and chemotaxis (Shimizu and Bray, 2002), all of which use computational tools in an attempt to understand mechanisms of cell regulation and control.

This study presents a computational simulation that includes allosteric regulation of the de novo pathway of pyrimidine biosynthesis. As opposed to standard kinetic models, this treatment considers temporal variations in the nutrient uptake and in concentration of allosteric effectors. This type of dynamic modeling allows the physiological adaptation of the cell, as evidenced in response of the nucleotide pools, to be evaluated. Not only is allosteric control of de novo pyrimidine biosynthesis simulated, but also the model formulation potentially allows for the prediction of differences in adaptation when the cells are grown under different environments.

The equations used to simulate the overall pathway response were tested individually and validated relative to existing literature data. In the case of the first reaction, which is catalysed by CPSase, the model accounts for the allosteric inhibition effected by UMP binding. In this simulation, saturation is achieved with comparable glutamine concentrations as has been

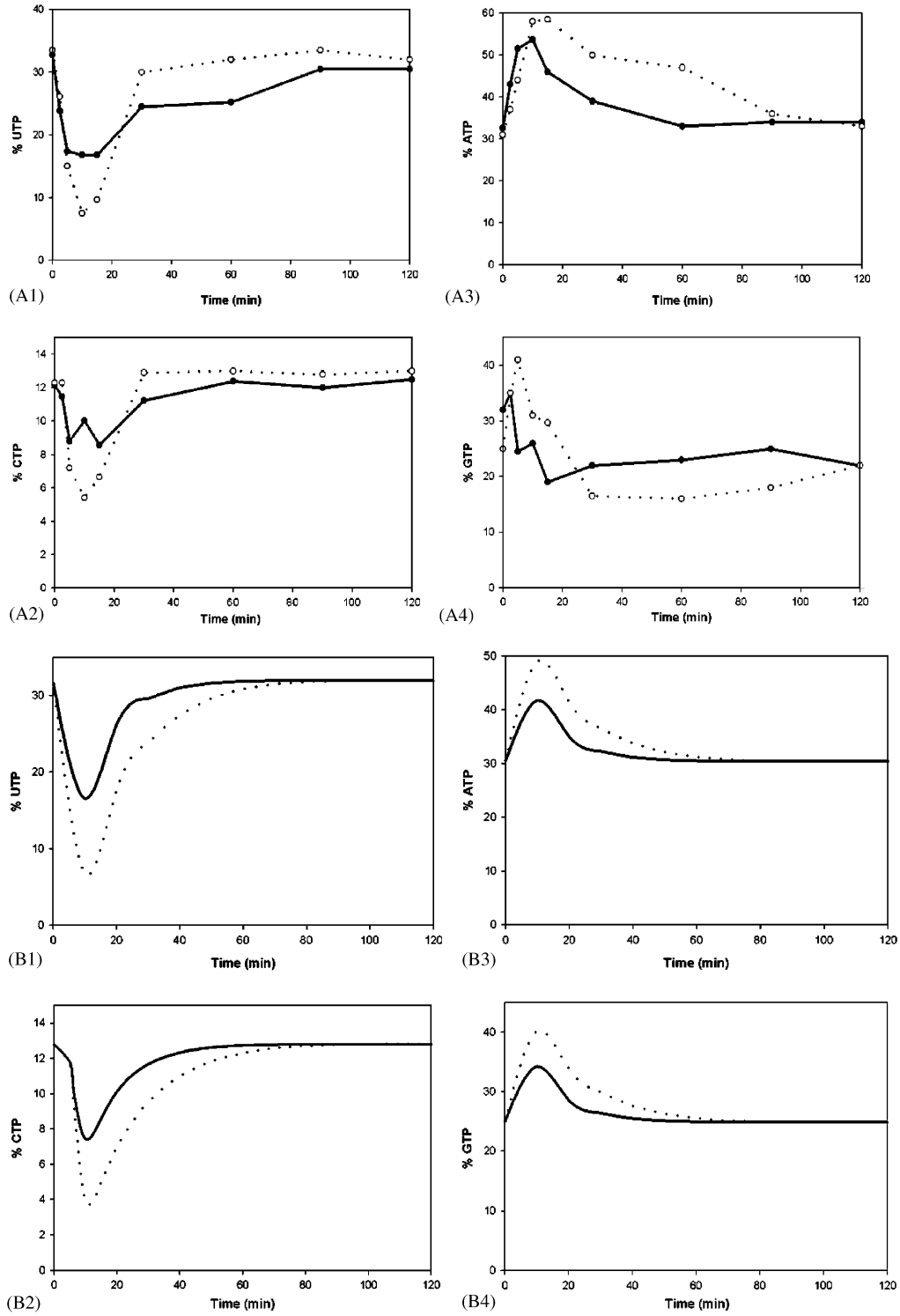

Fig. 5. Simulation of NTP pools response after pyrimidine pathway derepression. (A1–4) The experimental results reflect a sharp drop in the levels of CTP and UTP rapidly after derepression. (B1–4) The corresponding simulation shows remarkable similarity. Holoenzyme (—); catalytic subunit (· · · ·).

observed experimentally (Robin et al., 1989). The addition of uracil as an environmental variable and parameterization of the model yielded an optimal kinetic response.

A similar approach was utilized to evaluate the behavior of the model with respect to ATCase activity. The kinetic optimization in this case was more demanding, since the second enzyme of the pathway is

subject to the action of multiple homotropic and heterotropic controls. The critical step was to optimize the parameters and equations such that the regulatory lag caused by substrate cooperativity is seen as a sigmoidal path in a saturation curve. Multiple iteration steps had to be taken before each of the allosteric effects was simulated in agreement with the experimental observations from our laboratory. Successful simulation of the physiological response, including allosteric effects of the first two reactions, allowed us to simplify the addition of the remaining kinetic expressions and focus on the NTP levels as the objective of the refinement process.

The expression levels of the first two enzymes in the pathway were found to respond to the derepression simulation by a transient overexpression of CPSase, and an increase in steady-state levels in the case of ATCase. The timing and extent of these events correlated directly with the shift in the nucleotide pools. It is interesting to hypothesize about the roles of these two enzymes in the regulation of the flux through the metabolic pathway. CPSase levels respond to the concentration of its regulator UMP. ATCase levels rapidly build to increase the decaying levels of UMP and, ultimately, results in control of pyrimidine nucleotide homeostasis. CP, the product of the reaction catalysed by CPSase, is a highly unstable metabolite that, in addition, has to be partitioned between the pyrimidine and arginine biosynthetic pathways. While other organisms have multienzyme complexes that effectively channel this substrate through several catalytic sites (Lue and Kaplan, 1970; Williams et al., 1971; Coleman et al., 1977), this is not the case with *E. coli*. Studies performed with *Pyrococcus abyssi* provide an example of CPSase and ATCase that associate to form a transient complex or pseudo-compartment, thus facilitating transfer of the unstable CP produced from one catalytic site to the other (Purcarea et al., 1999). However, while there is evidence of substrate channeling in *E. coli* during protein synthesis, purine biosynthesis, carbohydrate phosphorylation through the phosphotransferase system and aspartic acid metabolism (Jakubowski, 1995; Rudolph and Stubbe, 1995; Rohwer et al., 1998; James and Viola, 2002), to our knowledge there are no reports of channeling involving pyrimidine metabolism. More recently, the process of metabolic channeling has been investigated in other biological systems using mathematical modeling (Maher et al., 2003), thus opening the door to the directed study of these and other metabolic control processes through computer simulations.

In the case of pyrimidine biosynthesis, integration of individual kinetics into the complete pathway required the development of a way to quantify the result of parameterization at each step of the metabolic pathway. Repression/derepression experiments have substantiated the role of the allosteric regulation in NTP pools consumption and production in *E. coli,* acting in concert with the important contribution of genetic control. The rapid drop in the observed CTP and UTP levels upon starvation for pyrimidines indicates the initial depletion of their intracellular concentrations, which was followed by a recovery as de novo biosynthesis of pyrimidines replenished the pools. The most sensitive component of this approach was the estimation of local minima used for the parametric calculations. Using a few selected parameters at a time, the sums of the squares of the residuals of the experimental data and the nucleotide fractions at specific times were calculated. Following this concept, the minimal set of parameters that were capable of capturing the allosteric response to uracil-induced repression/derepression was identified.

The initial drop in nucleotide pools corresponded to the depletion of pools as pyrimidine nucleotide synthesis shifted to the de novo pathway. Initially, the concentrations of CTP and UTP synthesized from uracil were sufficient to keep ATCase repressed. Immediately after uracil depletion, the NTP levels dropped. Allosteric inhibition and genetic repression were relieved and the activation of the enzyme was evidenced by the de novo synthesis of nucleotides as their pools stabilized at the normal physiological levels. Our model faithfully captured this behavior. In fact, the simulations showed the difference in the extent of the NTP levels responses between the holoenzyme and catalytic subunits that was observed experimentally. This demonstrated that the experimental results obtained for changes in CTP and UTP pool levels could be emulated by including allosteric parameters for CPSase and ATCase.

Even though the model proposed here is sufficient to approximate the allosteric responses in the de novo pyrimidine pathway, one would imagine that much of the control in vivo relies on the transcription of the *pyr* regulon. This model included a very simple mathematical formulation to modulate enzyme synthesis levels in response to pyrimidines; however, it is anticipated that additional parameters have to be defined and experimental data obtained that serve to validate those formulations, including measurements of intermediates. In addition, use of metabolic control analysis tools will yield valuable information about the contribution of each of the steps to the overall flux through the pathway and aid in developing and testing new hypotheses, such as those of metabolite channeling and pseudo-compartmentalization. A full model of the control of this pathway will contribute to the development and testing of hypotheses concerning the mechanisms used by the cell to regulate production of metabolites that are energy intensive. Our ability to make predictions of the outcomes of manipulating related cellular processes,

for application in medicine and biotechnology, should be greatly enhanced.

Acknowledgements

This research was supported by grants from the National Science Foundation (MCB 9723129) and the Robert A. Welch Foundation (A-915).

References

Allen, T.E., Herrgard, M.J., Liu, M., Qiu, Y., Glasner, J.D., Blattner, F.R., Palsson, B.O., 2003. Genome-scale analysis of the uses of the *Escherichia coli* genome: model-driven analysis of heterogeneous data sets. J. Bacteriol. 185, 6392–6399.

Alvarez-Vasquez, F., Canovas, M., Iborra, J.L., Torres, N.V., 2002. Modeling, optimization and experimental assessment of continuous L-(-)-carnitine production by *Escherichia coli* cultures. Biotechnol. Bioeng. 80, 794–805.

Beale, E.M.L., 1988. Introduction to Optimization. Wiley, New York, pp. 11–14, 25–36.

Bremer, H., Dennis, P., Ehrenberg, M., 2003. Free RNA polymerase and modeling global transcription in *Escherichia coli*. Biochimie 85, 597–609.

Christopherson, R.L., Finch, L.R., 1978. Response of the pyrimidine pathway of *Escherichia coli* K-12 to exogenous adenine and uracil. Eur. J. Biochem. 90, 347–358.

Coleman, P.F., Suttle, D.P., Stark, G.R., 1977. Purification from hamster cells of the multifunctional protein that initiates de novo synthesis of pyrimidine nucleotides. J. Biol. Chem. 252, 6379–6385.

Cornish-Bowden, A., 1997. New Beer in an Old Bottle: Eduard Buchner and the Growth of Biochemical Knowledge. Universitat de Valencia, Valencia, Spain, pp. 127–133.

Covert, M.W., Palsson, B.O., 2002. Transcriptional regulation in constraints-based metabolic models of *Escherichia coli*. J. Biol. Chem. 277, 28058–28064.

Forster, J., Famili, I., Fu, P., Palsson, B.O., Nielsen, J., 2003. Genome-scale reconstruction of the *Saccharomyces cerevisiae* metabolic network. Genome Res. 13, 244–253.

Hansen, F.G., Christensen, B.B., Atlung, T., 1991. The initiator titration model: computer simulation of chromosome and mini-chromosome control. Res. Microbiol. 142, 161–167.

Holden, C., 2002. Alliance launched to model *E. coli*. Science 297, 1459–1460.

Jakubowski, H., 1995. Proofreading in vivo. Editing of homocysteine by aminoacyl-tRNA synthetases in *Escherichia coli*. J. Biol. Chem. 270, 17672–17673.

James, C.L., Viola, R.E., 2002. Production and characterization of bifunctional enzymes. Substrate channeling in the aspartate pathway. Biochemistry 41, 3726–3731.

Jensen, K.F., Larsen, J.N., Schack, L., Sivertsen, A., 1984. Studies on the structure and expression of *Escherichia coli* pyrC, pyrD, and pyrF using the cloned genes. Eur. J. Biochem. 140, 343–352.

Koh, B.T., Tan, R.B., Yap, M.G., 1998. Genetically structured mathematical modeling of trp attenuator mechanism. Biotechnol. Bioeng. 58, 502–509.

Kramer, M., Bongaerts, J., Bovenberg, R., Kremer, S., Muller, U., Orf, S., Wubbolts, M., Raeven, L., 2003. Metabolic engineering for microbial production of shikimic acid. Metab. Eng. 5, 277–283.

Lee, S.Y., Hong, S.H., Moon, S.Y., 2002. In silico metabolic pathway analysis and design: succinic acid production by metabolically engineered *Escherichia coli* as an example. Genome Inform. Ser. Workshop Genome Inform. 13, 214–223.

LiCata, V.J., Allewell, N.M., 1997. Is substrate inhibition a consequence of allostery in aspartate transcarbamoylase? Biophys. Chem. 64, 225–234.

Lue, P.F., Kaplan, J.G., 1970. Metabolic compartmentation at the molecular level: the function of a multienzyme aggregate in the pyrimidine pathway of yeast. Biochim. Biophys. Acta. 220, 365–372.

Maher, A.D., Kuchel, P.W., Ortega, F., de Atauri, P., Centelles, J., Cascante, M., 2003. Mathematical modelling of the urea cycle. A numerical investigation into substrate channeling. Eur. J. Biochem. 270, 3953–3961.

Mulquiney, P.J., Kuchel, P.W., 2003. Modeling Metabolism with Mathematica. CRC Press, Boca Raton, FL, pp. 20–36.

Neidhardt, F.C., 1987. Chemical Composition of *Escherichia coli*. In: Neidhardt, F.C. (Ed. in chief), Ingraham, J.L., Low, K.B., Magasanik, B., Schaechter, M., Umbarger, H.E. (Eds.), *Escherichia coli* and *Salmonella typhimurium*. American Society for Microbiology, Washington, DC, p. 5.

Purcarea, C., Evans, D.R., Hervé, G., 1999. Channeling of carbamoyl phosphate to the pyrimidine and arginine biosynthetic pathways in the Deep Sea hyperthermophilic archaeon *Pyrococcus abyssi*. J. Biol. Chem. 274, 6122–6129.

Raghunathan, A., Price, N.D., Galperin, M.Y., Makarova, K.S., Purvine, S., Picone, A.F., Cherny, T., Xie, T., Reilly, T.J., Munson Jr., R., Tyler, R.E., Akerley, B.J., Smith, A.L., Palsson, B.O., Kolker, E., 2004. In silico metabolic model and protein expression of *Haemophilus influenzae* strain Rd KW20 in rich medium. OMICS 8, 25–41.

Reed, J.L., Palsson, B.O., 2004. Genome-scale in silico models of *Escherichia coli* have multiple equivalent phenotypic states: assessment of correlated reaction subsets that comprise network states. Genome Res. 14, 1797–1805.

Reed, J.L., Vo, T.D., Schilling, C.H., Palsson, B.O., 2003. An expanded genome-scale model of *Escherichia coli* K-12 (iJR904 GSM/GPR). Genome Biol. 4, R54.

Ricard, J., Cornish-Bowden, A., 1987. Co-operative and allosteric enzymes: 20 years on. Eur. J. Biochem. 166, 255–272.

Robin, J.P., Penverne, B., Hervè, G., 1989. Carbamoyl phosphate biosynthesis and partition of pyrimidine and arginine pathways of *Escherichia coli*. Eur. J. Biochem. 183, 519–528.

Rohwer, J.M., Postma, P.W., Kholodenko, B.N., Westerhoff, H.V., 1998. Implications of macromolecular crowding for signal transduction and metabolite channeling. Proc. Natl Acad. Sci. USA 95, 10547–10552.

Rubino, SD., Nyunoya, H., Lusty, CJ., 1986. Catalytic domains of carbamyl phosphate synthetase. J. Biol. Chem. 261, 11320–11327.

Rudolph, J., Stubbe, J., 1995. Investigation of the mechanism of phosphoribosylamine transfer from glutamine phosphoribosylpyrophosphate amidotransferase to glycinamide ribonucleotide synthetase. Biochemistry 37, 2241–2250.

Schilling, C.H., Covert, M.W., Famili, I., Church, G.M., Edwards, J.S., Palsson, B.O., 2002. Genome-scale metabolic model of *Helicobacter pylori* 26695. J. Bacteriol. 184, 4582–4593.

Schlosser, P.M., Bailey, J.E., 1990. An integrated modeling-experimental strategy for the analysis of metabolic pathways. Math. Biosci. 100, 87–114.

Segre, D., Zucker, J., Katz, J., Lin, X., D'Haeseleer, P., Rindone, W.P., Kharchenko, P., Nguyen, D.H., Wright, M.A., Church, G.M., 2003. From annotated genomes to metabolic flux models and kinetic parameter fitting. OMICS 7, 301–316.

Shimizu, T.S., Bray, D., 2002. Modelling the bacterial chemotaxis receptor complex. Novartis Found. Symp. 247, 162–177.

Vilar, J.M., Guet, C.C., Leibler, S., 2003. Modeling network dynamics: the lac operon, a case study. J. Cell. Biol. 161, 471–476.

Wales, M.E., Wild, J.R., 1999. Aspartate transcarbamoylase. In: Creighton, TE. (Ed.), Encyclopedia of Molecular Biology. Wiley, New York, pp. 196–201.

Wales, M.E., Mann-Dean, M.G., Wild, J.R., 1988. Characterization of pyrimidine metabolism in the cellular slime mold, *Dictyostelium discoideum*. Can. J. Microbiol. 35, 432–438.

Wild, J.R., Loughrey, S.J., Corder, T.C., 1989. In the presence of CTP, UTP becomes an allosteric inhibitor of aspartate transcarbamoylase. Proc. Natl Acad. Sci. USA 86, 52–56.

Williams, L.G., Bernhardt, S.A., Davis, R.H., 1971. Evidence for two discrete carbamyl phosphate pools in Neurospora. J. Biol. Chem. 246, 973–978.